

Gianfranco Bocchinfuso\*, Claudia Mazzuca, Paolo Conflitti,  
Davide Cori, Tommasina Coviello, and Antonio Palleschi

# Relative Stability of the Scleroglucan Triple-Helix and Single Strand: an Insight from Computational and Experimental Techniques

DOI 10.1515/zpch-2015-0734

Received November 10, 2015; accepted May 4, 2016

**Abstract:** Scleroglucan (Sclg) is a polysaccharide that exhibits a triple helix conformation (triplex), both in aqueous solution and in the solid state, which is lost in DMSO solution, at high temperature and at high pH values. The triplex conformation is characterized by a high rigidity, responsible of Sclg peculiar properties. Although the relative stability of triplex and single strand has already been investigated, different structural details are still missing.

In the present study, we analyse the structural properties and the factors stabilizing the single chain and the triple helix of Sclg in different conditions. To this end, we simulated both systems in water and in DMSO. The triple helix has been also simulated in the presence of chemical damages on one of the three strands (to reproduce *in silico* the effect of sonication) or by inducing a partial unfolding of the triplex structure. The computational results have been compared with experimental evidences in which the triplex denaturation, at alkaline pH values, has been followed by monitoring the UV and CD spectra of Congo red, used as a probe molecule. Our results indicate that sonication breaks the Sclg chains without appreciably changing the stability of the other tracts of triple helix. The simulated perturbed or partially unfolded triplexes show a clear tendency to form less

---

**Article Note:** Gianfranco Bocchinfuso and Antonio Palleschi contributed equally to this work.

---

**\*Corresponding author: Gianfranco Bocchinfuso**, Dipartimento di Scienze e Tecnologie Chimiche, Università di Roma Tor Vergata, Rome, Italy,  
e-mail: [gianfranco.bocchinfuso@uniroma2.it](mailto:gianfranco.bocchinfuso@uniroma2.it)

**Claudia Mazzuca, Paolo Conflitti, Davide Cori, Antonio Palleschi:** Dipartimento di Scienze e Tecnologie Chimiche, Università di Roma Tor Vergata, Rome, Italy

**Tommasina Coviello:** Dipartimento di Chimica e Tecnologie del Farmaco, Università degli studi di Roma “La Sapienza”, Rome, Italy

ordered aggregates. Finally, our simulations put in evidence an important role of the hydrophobic interactions both in the triplex stability and in the aggregation processes observed after induced denaturation.

**Keywords:** Triplex Scleroglucan, Single Strand Scleroglucan, Molecular Dynamics Simulations, Congo Red, Hydrophobic Effect, Induced CD.

## 1 Introduction

Scleroglucan (ScIg) is a polysaccharide secreted by fungi of the genus *Sclerotium*. It exhibits a backbone built up by  $(1 \rightarrow 3)$  linked  $\beta$ -D-glucopyranose (glcp) side chains linked  $\beta$ -( $1 \rightarrow 6$ ) to every third residue in the main chain. Like other polysaccharides with a similar structural organization, ScIg exhibits a triple helix conformation (triplex) in a wide range of conditions, from water solutions [1] to solid state [2]. The triplex stability is attributed to a network of interchain H-bonds among the hydroxyl groups linked to the C-2 atoms of the glucose units of the backbone [3]. Triplex conformation is responsible for the ScIg peculiar properties, in comparison with other polysaccharides, mainly due to its high stiffness. For this reason, ScIg has been successfully used for different industrial applications (secondary oil recovery, ceramic glazes, food, paints, cosmetics, etc.) [4], as well as a matrix for controlled drug release [5]. In this context, it is important to investigate the stability of the triplex in comparison to the single strand conformation (ss-ScIg). It is known that the ScIg triplex is stable in water solution up to 135 °C. Furthermore, triplex stability decreases by adding DMSO to the water solution, or by increasing the alkalinity, with a triplex unfolding observed close to pH 13 [6–8]. Very similar behaviours have been reported for other  $(1 \rightarrow 3)$ - $\beta$ -D-glucans with 1,6-linked branches, from a structural point of view, closely related with ScIg [9–12]. The reversibility of the triplex to ss-ScIg transition is still under discussion; however, in many experimental conditions, the native triplex does not form again after a denaturation process occurred [13–15].

In the last decade, by using both experimental and computational techniques, we investigated the drug release properties of tablets formed by ScIg, also in the presence of borax [3, 5, 16–21]. During the water uptake process, a gel phase forms and the release of the drugs is related to their diffusion into the gel. Borax favours the parallel configuration of nearest neighbour triplexes through chemical/physical bonds. This alignment induces the formation of a sort of channels, whose boundaries are defined by physically joined triplexes. We named these superstructures “soft-nanochannels”, whose properties are due to the intrinsic rigidity of the triplexes; in particular, we have shown that their presence

strongly influences the drug release. On the other hand, from a structural point of view, only few information are known about the ss-ScIg, as well as on the triplex unfolding process.

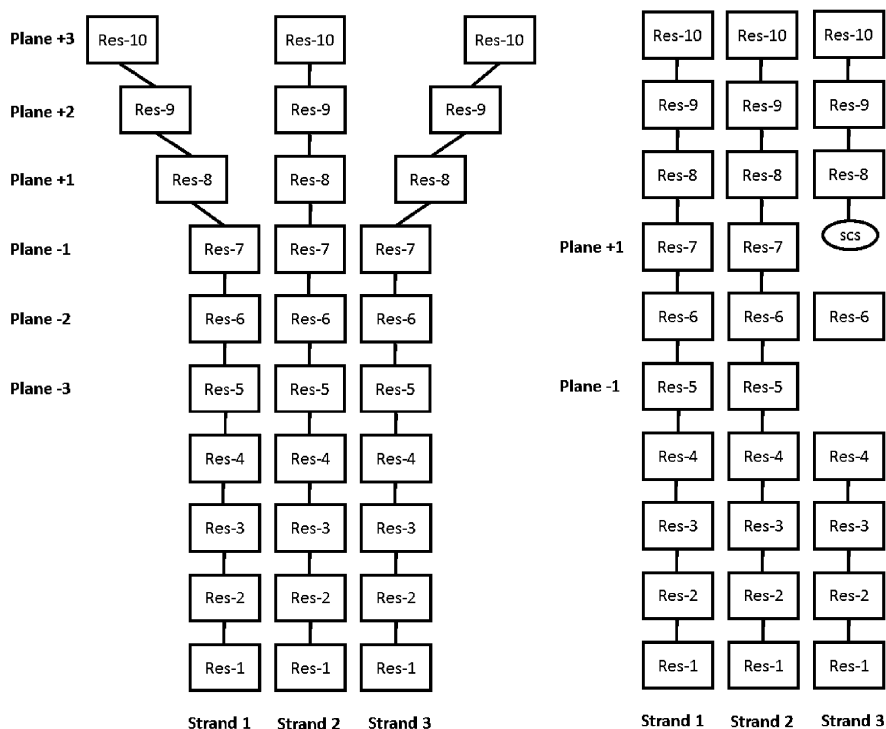
It is known that the interaction between ScIg triplex and Congo red (CR) produces a shift in the CR absorption band and, more interestingly, induces a circular dichroism (CD) signal [22–26]. This signal is lost when triplex unfolds, suggesting that after denaturation ScIg loses the triplex configuration, but the structural details on the ScIg/CR complexes are still missing. The limited structural characterization of these phenomena is also due to the different problems faced when studying the three-dimensional details of polysaccharides, e.g. many of them do not crystallize, their NMR signals are highly overlapped and the NMR spectra frequently contain second order line-shaped resonances [27]. Thus, it is usual to use computational techniques, as a complement of the experimental data, in order to obtain structural information. Ten years ago, for the first time, molecular dynamics simulations were applied by us to investigate the triplex at low and room temperature, to discuss its high stability, and to clarify the role of water molecules in the mobility of glucose rings in the ScIg side chains, involved in a conformational transition occurring at around 7 °C [3]. MD simulations were also applied to show that the presence of borax does not change the intrinsic features of triplexes [18, 19], while an opposite behaviour was observed in the case of the intrinsically disordered polysaccharides guar gum [21].

In this paper the factors leading to the stability of ss-ScIg and triplex in different conditions are discussed. In particular, ss-ScIg has been simulated both in DMSO (where it is stable) and in water (where, on the opposite, the triplex is stable). Furthermore, the triplex stability after sonication has been investigated by means of experimental and computational techniques. In particular, the triplex denaturation has been experimentally monitored by following the perturbation induced on the spectroscopic properties of CR (UV and CD spectra). In the final part of the paper, the results of MD simulations carried out on the ScIg/CR complexes are also presented.

## 2 Materials and methods

### 2.1 MD simulations

MD simulations were carried out by using the software package Gromacs v4.6.5 [28]. The force field parameters for ScIg were those already used in a previous work [3], while for CR the parameters were taken from Krol et al. [29]. The



**Scheme 1:** Graphical representation of the starting structure used in the MD simulations of partially unfolded (on the left) and sonicated (on the right) triplexes. Each rectangle represents a ScIg repeating unit (three glucose rings in the backbone and one glucose ring in the sidechain). Each strand contains an additional glucose ring at the terminal O-1; for sake of clarity these residues are not reported in the scheme, except in one case, where it is represented as a circle. The structures represent a triplex after a physical or a chemical perturbation, respectively.

systems were simulated in triclinic or cubic boxes with different dimensions, in a NPT ensemble. Electrostatic interactions were calculated with the PME algorithm [30] (cut-off 14 Å) and a double cut-off was used for the van der Waals interactions (10–14 Å). Pressure and temperature were kept constant by using the Berendsen algorithm [31]. In the case of simulations in the presence of CR, two sodium ions were added to assure the electroneutrality.

After minimization, the systems were simulated at 50 K for 100 ps and then heated to 300 K with a 700 ps long stepwise protocol. All systems were first equilibrated at 300 K for 200 ps. In all cases, the simulations were carried out in explicit water [32] and DMSO [33] solutions and the terminals were capped with a glucose

ring at the terminal O–1 and a methoxyl group at the terminal O–3, with the exception of the single ScIg monomer simulation (res 6 in strand 3, Scheme 1, right).

In the simulations with single strand (20 ns long), the ScIg chain was built with ten ScIg repeating units.

The triplex renaturation started from a structure partially unfolded with ten residues for each chain. To obtain this structure, for each strand, the value of the inter-ring torsional angles ( $\varphi$  and  $\psi$ ) connecting the ScIg residues 7 and 8 was changed. The assigned values for the three pairs (one for each strand) were those corresponding to one of the two local minima identified in the MD simulation of the laminarabiose, the (1  $\rightarrow$  3) linked  $\beta$ -D-glcp dimer (Figure 3 in Reference [3]). The final effect was a structure in which the first seven residues of each chain were assembled in a regular triplex while the remaining three ScIg residues were unfolded and far from each other, in an *umbrella-like* structure (Scheme 1, left). This system was simulated in both water and DMSO for 42 ns. In this case, an annealing protocol was also applied, with temperatures changing between 300 and 450 K in ten cycles.

The interaction with CR was investigated by simulating a seven residues ss-ScIg and a triplex composed by three strands, each composed by seven ScIg residues. Three and six independent simulations were acquired for ss-ScIg and triplex, respectively. The starting configurations were prepared with CR at different random distances (higher than 1 nm) and orientations with respect to the polysaccharide. The total simulation time was 240 ns for CR and ss-ScIg and 400 ns for CR and triplex.

Solvent Accessible Surface (SAS), Root Mean Square Fluctuation (RMSF), H-bond evaluation, and the clusterization were obtained by using the tools of the GROMACS software package. In particular, *g\_cluster* was used also to obtain the more representative structure in the clusters, which it is defined as the structure with the smallest average distance to the other ones within the cluster.

The structural images were obtained by using the software Chimera [34] or VMD, developed with NIH support by the Theoretical and Computational Biophysics group at the Beckman Institute, University of Illinois at Urbana-Champaign.

## 2.2 CD and UV experiments

ScIg (Actigum<sup>TM</sup> Cs) was purchased from Cargill (Cargill, MN, USA), and the other reagents from Sigma (Sigma-Aldrich, Mo, St. Louis, USA). ScIg samples were purified and sonicated as previously reported [35]. The average molecular weight of ScIg was determined by viscometric measurements according to

the Mark–Howink–Sakurada equation [36]. UV and CD experiments were carried out on solution of ScIg sonicated for different period of time, 7 ( $t = 0$  min, ScIg MW =  $1.0 \cdot 10^6$  amu;  $t = 10$  min, ScIg MW =  $5.5 \cdot 10^5$  amu;  $t = 90$  min, ScIg MW =  $2.7 \cdot 10^5$  amu).

The solutions at different pHs were prepared by adding appropriate aliquots of a NaOH stock solution (10 M) to ScIg solutions (1 g/l) containing 10  $\mu$ M of CR. The solutions were left to stabilize for 30 min before recording the UV-Vis and CD spectra. For an appropriate comparison, all spectra were recorded also on a 10  $\mu$ M CR solution. The absorption spectra were recorded by using a Cary 100 spectrophotometer (Varian, Palo alto, CA, USA), whilst CD spectra were acquired on a Jasco J-600 apparatus. In both cases, quartz cuvettes (1 cm path length) were used.

## 3 Results and discussions

### 3.1 Scleroglucan single strand in water and DMSO

As mentioned above, high concentrations of DMSO ( $> 85\%$  v/v) lead to the triplex denaturation. To elucidate the effects of different environments, ss-ScIg MD simulations have been carried out in only water or pure DMSO. As starting structure, a single extended strand, taken from a triplex previously simulated, were used [3]. Figure 1 reports the more representative conformations of the two simulations.

In DMSO, the starting (extended) conformation of ss-ScIg remains stable during the simulation time (Figure 1A). On the other hand, in water the ss-ScIg undergoes a structural transition after roughly 8 ns assuming a more compact conformation (Figure 1B). This transition is promoted by an unusual deformation of one of the glucose rings in the ss-ScIg backbone (Figure 1C). This ring first assumes a boat-like conformation and after less than 2 ns adopts the  ${}^1C_4$  conformation, where all substituents are in the axial position with respect to the glucose plane. Figure 2 (top) reports the value of two opposite torsional angles in this ring during the simulation. After a transition from  $+60^\circ$  to  $-60^\circ$  of one of them, the second one undergoes an opposite transition after ca 2 ns. In order to individuate the driving force of this transition, the SAS of the carbon atoms of the glucose rings in the backbone has been investigated. In the glucose  $\beta(1 \rightarrow 3)$  linkage, these carbons are slight shielded by the hydroxyl groups. The SAS values calculated in the DMSO simulation do not significantly change while, in water, when the folding occurs, a noticeable decrease of the SAS values is observed (Figure 2, bottom).

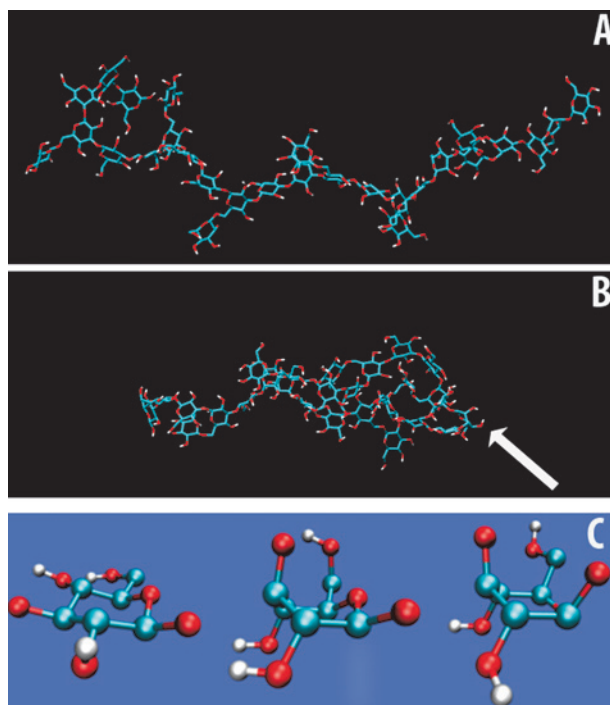


**Figure 1:** More representative structures of the MD simulations of ss-Sclg in DMSO (A) and in water (B), as obtained by using the g\_cluster tool in GROMACS. The arrow in the panel B indicates the glucose ring in the hinge point. The panel C reports, from left to right, the structures of this ring before, during and after the transition, which leads to the folded structure.

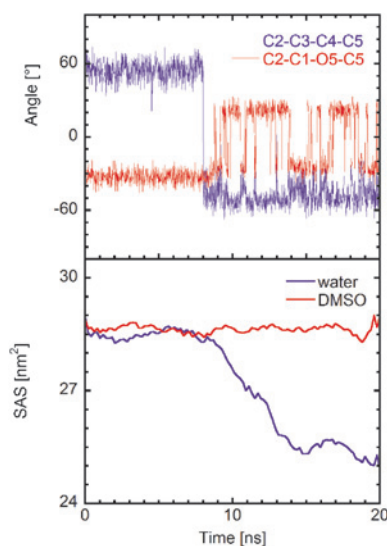


**Figure 2:** Top: time-evolution, during the MD simulation of ss-Sclg in water, of two intra-ring torsional angles of the glucose residue indicated with an arrow in Figure 1. Bottom: time evolution of the SAS values, obtained in the MD simulations of ss-Sclg in water (blue curve) and DMSO (red curve), for the Carbon atoms (C1, C2, C3, C4 and C5) belonging to the glucose rings of the Sclg backbone.

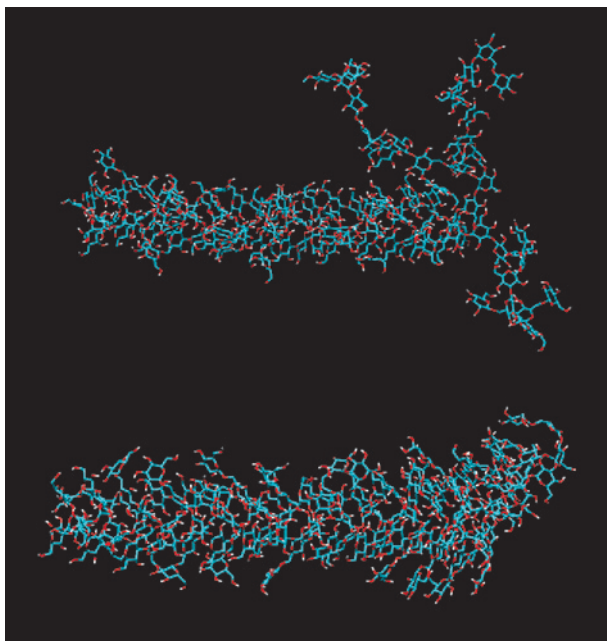


**Figure 3:** Final structures from the MD simulations of the partially unfolded triplex in DMSO (top) and water (bottom).

### 3.2 Triplex renaturation

To investigate the tendency to form ordered aggregates of ScI<sub>g</sub>, we induced a partial denaturation in the last three residues of a triplex built with ten repeating units for each strand (Scheme 1). The refolding tendency of the structure has been investigated by means of two simulations of 42 ns in water and DMSO, with the temperature changing between 300 and 450 K. The final structures of the simulations are reported in Figure 3. We performed also two further independent simulations in which the temperature was kept constant at 300 K; the results of these simulations (not reported) were not significantly different from those here presented.

In the simulation carried out in DMSO the structure remains similar to the starting one, as no tendency to refold is evident during the simulation time, and the three unfolded arms remain completely solvent exposed (Table 1). Moreover, no tendency to further unfolding is registered, while the experimental evidences indicate the triplex denaturation in these conditions. This is probably due to the short simulation time, in comparison with the time required for the complete triplex unfolding. A different behaviour is observed when the same structure is simulated in water. In this case, the three segments, open in the starting conformation, immediately interact with each other and form a folded structure. At the



**Table 1:** SAS values from the MD simulations starting from a partially unfolded triplex in water and in DMSO.

|                          | DMSO [nm <sup>2</sup> ] |                                 |                      | Water [nm <sup>2</sup> ] |                                 |                      |
|--------------------------|-------------------------|---------------------------------|----------------------|--------------------------|---------------------------------|----------------------|
|                          | start <sup>1</sup>      | 5 <sup>th</sup> ns <sup>1</sup> | last ns <sup>1</sup> | start <sup>1</sup>       | 5 <sup>th</sup> ns <sup>1</sup> | last ns <sup>1</sup> |
| SAS <sub>(plane+1)</sub> | 3.43                    | 3.5 ± 0.2                       | 3.1 ± 0.2            | 3.59                     | 0.4 ± 0.1                       | 0.5 ± 0.1            |
| SAS <sub>(plane+2)</sub> | 3.96                    | 4.1 ± 0.2                       | 3.7 ± 0.2            | 4.03                     | 1.1 ± 0.1                       | 1.0 ± 0.2            |
| SAS <sub>(plane+3)</sub> | 4.06                    | 3.7 ± 0.2                       | 3.8 ± 0.2            | 4.16                     | 1.2 ± 0.1                       | 1.2 ± 0.1            |

<sup>1</sup> The values reported in the columns “start”, “5<sup>th</sup> ns” and “last ns” refer to the SAS measured in the first frame of the simulations, the average value obtained between 4 ns and 5 ns, and between 41 and 42 ns, respectively.

same time, a noticeable reduction of the SAS value of the hydrophobic region in the backbone is detected (Table 1). To investigate the similarity between the obtained folded structures and the native triplex, the number of H-bonds between the hydroxyl groups in position 2 on the glucose ring in the backbone, which are directly involved in the stability of the triplex arrangement, has been measured. With more details, we have compared the average number of the H-bonds measured in the refolded tract (planes +1, +2 and +3) in the last ns of simulation with the number of H-bond observed in the plane −3, never unfolded during the simulation time (see Scheme 1). The percentage of the number of H-bonds measured for plane +1, +2 and +3 respect to that of the plane −3 has been  $17 \pm 11$ ,  $8 \pm 8$  and  $28 \pm 11$ , respectively. These results indicate that the sampled conformations assure a good shielding for the hydrophobic regions, but they are different from the well-ordered structure characterizing the native triplex. The difficulty in obtaining again the native triplex structure, observed in our simulations, is in agreement with the experimental evidences reported by Stokke and co-workers, which showed that triplex refolding is difficult once the denaturation occurred [13–15].

### 3.3 Effect of sonication

#### 3.3.1 Simulation of “chemically” degraded triplex

Previous works have shown that sonication reduces the molecular weight of triplex, but the structural effects on the triplex were not fully investigated [35]. Stokke and co-workers estimated that, in order to disentangle a triplex, in one of the three chains double cuts close to each other must occur [37].

To mimic these conditions, we have simulated a triplex decamer modified as reported in the Scheme 1 (right) both in water and in DMSO solution. One of the

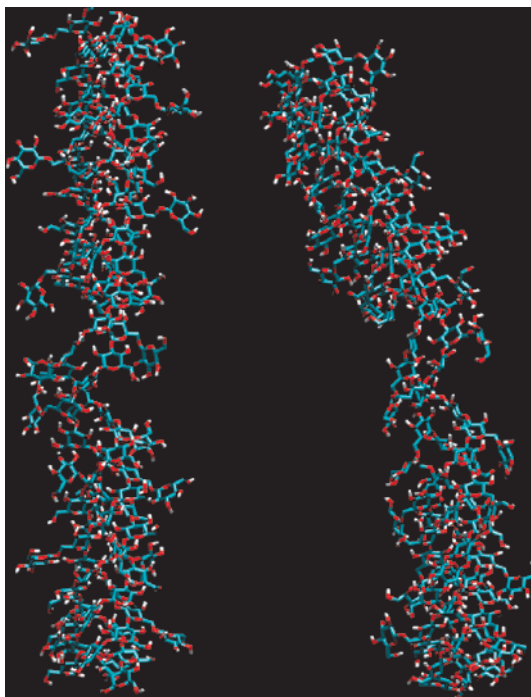


**Figure 4:** Final structure obtained after the pull-dynamic simulations in water.

three strands was split in three different molecules, composed by 4, 1 and 3 ScIg residues, respectively. A harmonic potential was applied to pull away the ScIg monomer (Res 6 in Scheme 1) from the triplex. The obtained structure in water solution is reported in Figure 4. A bending of the triplex axis is evident, with the hinge point corresponding to the region where the ScIg monomer was eliminated.

The SAS of the hydrophobic atoms of the residues, indicated as plane +1 and plane -1 for the strands 1 and 2 in the Scheme 1, has been calculated. The average value in the last ten ns of the simulations, when the ScIg monomer does not interact with the remaining part of the saccharidic moiety, was  $1.6 \pm 0.2 \text{ nm}^2$ , very close to the value obtained at the early beginning of the simulation ( $1.4 \pm 0.1 \text{ nm}^2$  in the first 100 ps), when these residues faced the ScIg monomer. For comparison, in DMSO solution the same value increases from  $1.4 \pm 0.1 \text{ nm}^2$  (in the first 100 ps) to  $2.5 \pm 0.2 \text{ nm}^2$  (in the last ten ns). Once again, a shielding of the hydrophobic region correlates with the structural transition, in this case by limiting the solvent accessibility on the residues potentially exposed after the monomer removal.

Interestingly, the regions of the triplex that are not directly involved in the introduced “chemical” damages remain stable, in spite of the significant reduction of the number of Slgc monomers in the residual tracts.

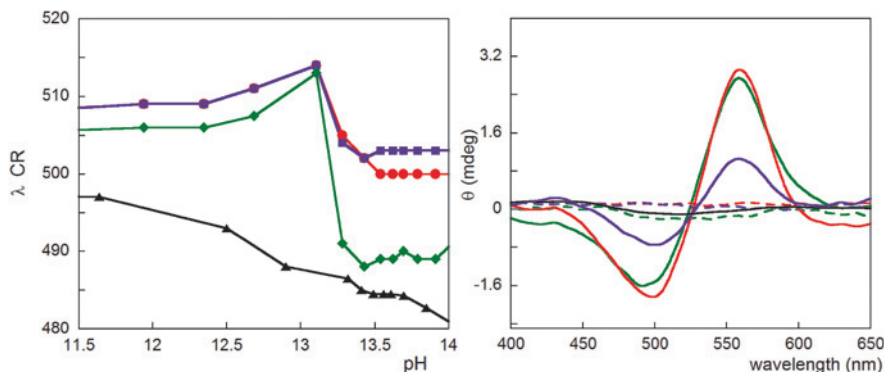


**Figure 5:** Left: Wavelength of the maximum of the absorbance in the UV CR spectra in water solution in the absence and in the presence of Sclg. Right: CD spectra of CR in the absence and in the presence of Sclg at pH 14 (dashed line) and 8 (continuous lines) in water solution. The different colours refer to CR solution (dark) Sclg (green) and Sclg sonicated for 10 (red) and 90 min (blue).

### 3.3.2 UV and CD spectra of Congo red in the presence of scleroglucan

CR is a well-known probe, which is used to follow structural transitions in biomacromolecules, including polysaccharides [22–24]. Changes in the surrounding conditions (e.g., due to interactions with other molecules) determine a detectable shift in the maximum of the CR absorption spectrum. More interestingly, CR may show an induced CD signal if the interaction takes place with ordered macromolecules [25, 26]. We have used these CR properties to follow the triplex denaturation in the unperturbed Sclg and after sonication. Figure 5 reports the obtained results.

The UV spectra of CR in the presence of Sclg show a blue shift of the maximum at pH 13, regardless of the sonication time (Figure 5, left). This behaviour is not observed in the CR spectra (Figure 5). In this case, the maximum shows a slight negative drift by increasing the pH values, without transitions, accordingly to Faríña et al. [23]. The extent of the shift at pH 13 in the presence of Sclg decreases with the sonication time. The CD spectra, corresponding to the absorption band of CR, have been also acquired at pH 8 and 14. At pH 8, in the absence of Sclg, CR does not show any CD signal. On the other hand, a well-defined band is present in all the samples where Sclg is present. For the Sclg sample sonicated for 90 min, a lower induced CD signal is registered, in agreement with the different blue shift extent of the UV spectra recorded in the same conditions. In all the samples, the CD signal is lost at pH 14 (Figure 5, right). These data confirm that a structural transition between an ordered (triplex) and a disordered (ss-Sclg) state takes place at pH 13.

The different extent of the blue shift and the lower intensity of the CD spectra show that Sclg is sensitive to the sonication process. It can be speculated that the degradation of Sclg, promoted by sonication, lowers the total amount of triplexes present in solution after sonication; however, the sonication does not change the pH of the transition. Overall, this suggests that the chemical damages due to sonication (leading to a decrease in the MW) slightly affect the stability of the triplex tracts. This is in agreement with the MD results, above discussed, showing that also a severe chemical damage of one of the three chains does not significantly affect the stability of the residual triplex.

### 3.3.3 Congo red-scleroglucan interaction

The data reported in the previous paragraph confirm that the interaction with Sclg leads to an induced CD on the CR only in the case of the triplex conformation. The absence of CD signal with ss-Sclg could be due to a small binding constant or to a low degree of order in the formed complex. To elucidate these aspects and to give a structural view of these complexes, MD simulations of CR in the presence of ss-Sclg (three independent simulations) and triplex (six independent simulations) have been carried out. Only the portions of trajectory in which CR was in contact with the polysaccharide chains were analysed, for a total amount of 150 ns, both for triplex and for ss-Sclg. In both cases, stable interactions between Sclg and CR take place. The triplex results stable and the presence of CR does not introduce an appreciable distortion from the starting (well-ordered) structure. This is in agreement with the high stability of triplex already observed in the presence of external stimuli in different conditions; for example, only a slight perturbation in the mobility of the glucose side chains has been recorded for the triplex linked to borax groups [18, 19]. On the other hand, as already observed in the case of ss-Sclg alone, the single strand is flexible, and different conformations were sampled during the simulations. These data are in agreement with the fluorescence correlation spectroscopy results showing that at pH greater than 13 ss-Sclg adopts random coil conformations [38]. In this context, the presence of CR *per se* seems to be not able to introduce an increasing in the order of the single chain. The RMSF calculated during the analysed 150 ns of simulation on the C-1 atoms of the glucose ring in the Sclg backbone has been  $0.67 \pm 0.13$  and  $0.15 \pm 0.04$  nm for ss-Sclg and triplex, respectively. This different behaviour of the polysaccharidic moiety led to a different interaction with the CR molecules. In the simulation of the CR-triplex, two configurations represent the 74% of the analysed simulation time. These structures, reported in Figure 6, show a different orientation for CR molecules with respect to the triplex helical axis. It is difficult, taking into account only the data of the

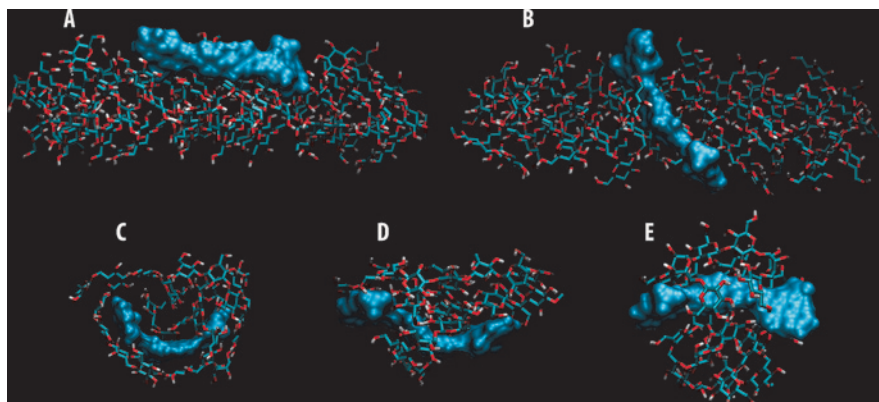


**Figure 6:** More representative structures of the MD simulations of CR in the presence of triplex and ss-Sclg, as obtained by using the `g_cluster` tool of GROMACS. In the former case, the two more populated clusters from six independent simulations are reported (panel A and B). In the case of simulations with ss-Sclg the more representative structures of three independent simulations are reported (panel C–E). In all the cases, Sclg is reported as stick colored by atoms and CR as a cyan surface.

present simulations, to predict the relative stability of these configurations; however, in both cases they are stable, once they are populated. Based on the high order of the triplex, it can be speculated that both these configurations can lead to the induced CD signals. On the opposite, in the three simulations with ss-Sclg, different configurations were sampled; for this reason, the three simulations have been independently clustered. Figure 6 shows the more representative structures obtained from the clusterizations of the last 50 ns of the three simulations. Due to the high conformational fluctuations, these structures cannot be considered as representative of the configurations explored during the three simulations; indeed, a high value of the cut-off parameter in `g_cluster` (2.5 nm) has been needed to obtain one cluster for each simulation. The high fluctuations observed, explain the absence of an induced signal in the CD spectra.

## 4 Conclusions

Sclg owes its properties to the unusual triple helical conformation assumed in water solution; for this reason, the equilibrium between triplex and ss-Sclg has been deeply investigated in the last decades. In this work, MD techniques have been applied to simulate both systems in different conditions, to give a structural picture

of the features leading to the peculiar conformation of this polysaccharide. It is known that the triplex, in water solutions, is stable at pH values lower than 13 and it unfolds at higher values. In this work, it is shown that the pH of the ScIg transition is unchanged also after sonication. To this end, UV and CD spectra of CR in the presence of ScIg at different pH values have been reported. These results confirm the stability of the triplex conformation, also in the presence of strong perturbations. These experimental evidences are in good agreement with the results obtained with MD simulations, which clearly show that even short tracts of triplex are stable after a physical denaturation or chemical damages. Furthermore, most of the transitions observed in the simulations indicate a strong tendency of ScIg to shield the carbon atoms in the glucose rings of the backbone. The peculiar position of the hydroxyl groups in the glucose and the inter-ring linkage  $\beta(1 \rightarrow 3)$  leave these atoms more exposed to the solvent, conferring to this region a weak hydrophobic character. The triplex conformation, on the other way, assures a tight contact between these regions and minimize their accessibility to the solvent molecules.

The importance of the hydrophobic interactions is particularly clear when the single strand is simulated in water solution. In this case, the single strand undergoes a conformational transition to minimize the SAS of the plane formed by C atoms in the glucose ring. When the starting structure was a partially unfolded triplex, interactions between the three strands arise once again correlated with a decreasing in the exposition of the ScIg hydrophobic region. However, a refolding of a native triplex has not been observed, in agreement with the experimental evidences. Overall, these data indicate that the hydrophobic interactions play an essential role in the stabilization of the triplex, which add to the well-known stabilizing effect played by the inter-strands H-bonds involving the O-2 hydroxyl groups in the backbone.

Finally, to the best of our knowledge, a structural picture of the complexes formed by CR and ScIg, both in the triplex and in the ss-ScIg conformation it has been proposed for the first time. The simulations reported in the paper show that in the former case well-ordered complexes are formed, in agreement with the experimental evidence of an induced CD signal in the CR spectrum, when ScIg triplexes are present. On the other hand, CR interacts with ss-ScIg, but the formed complex is not ordered enough to induce a dichroic signal.

**Acknowledgement:** We acknowledge the CINECA award under the ISCRA initiative, for the availability of high performance computing resources and support.

## References

1. T. Norisuye, T. Yanaki, and H. Fujita, *J. Polym. Sci. Polym. Phys.* **18** (1980) 547.
2. L. T. Bluhm, Y. Deslandes, R. H. Marchessault, S. Perez, and M. Rinaudo, *Carbohydr. Res.* **100** (1982) 117.
3. A. Palleschi, G. Bocchinfuso, T. Coviello, and F. Alhaique, *Carbohydr. Res.* **340** (2005) 2154.
4. I. Giavasis, L. M. Harvey, and B. McNeil, *Scleroglucan*, in: *Biopolymers*, Volume 6, *Polysaccharides II: Polysaccharides from Eukaryotes*, S. De Beats, E. J. Vandamme, A. Steinbuchel (Eds.), Wiley-VCH, Weinheim (2002) 37.
5. T. Coviello, A. Palleschi, M. Grassi, P. Matricardi, G. Bocchinfuso, and F. Alhaique, *Molecules* **10** (2005) 6.
6. S. Kitamura, T. Hirano, K. Takeo, H. Fukada, K. Takahashi, B. H. Falch, and B. T. Stokke, *Biopolymers* **39** (1996) 407.
7. S. Kitamura and T. Kuge, *Biopolymers* **28** (1989) 639.
8. S. C. Viñarta, O. D. Delgado, L. I. C. Figueroa, and J. I. Fariña, *Carbohydr. Polym.* **94** (2013) 496.
9. F. Qin, F. L. Aachmann, and B. E. Christensen, *Carbohydr. Polym.* **90** (2012) 1092.
10. Q. Liu, X. Xu, and L. Zhang, *Biopolymers* **97** (2012) 988.
11. F. Qin, M. Sletmoen, B. T. Stokke, and B. E. Christensen, *Carbohydr. Polym.* **92** (2013) 1026.
12. K. Yoshiba, T. Sato, T. Osumi, A.-S. T. Ulset, and B. E. Christensen, *Carbohydr. Polym.* **134** (2015) 1.
13. B. T. Stokke, S. Kitamura, and A. Elgsaeter, *Int. J. Biol. Macromol.* **15** (1993) 63.
14. M. Sletmoen and B. Stokke, *Biopolymers* **89** (2008) 310.
15. T. McIntire and D. Brant, *J. Am. Chem. Soc.* **120** (1998) 6909.
16. T. Coviello, F. Alhaique, C. Parisi, P. Matricardi, G. Bocchinfuso, and M. Grassi, *J. Control. Release* **102** (2005) 643.
17. T. Coviello, M. Grassi, A. Palleschi, G. Bocchinfuso, G. Coluzzi, F. Banishoeib, and F. Alhaique, *Int. J. Pharm.* **289** (2005) 97.
18. A. Palleschi, T. Coviello, G. Bocchinfuso, and F. Alhaique, *Int. J. Pharm.* **322** (2006) 13.
19. G. Bocchinfuso, A. Palleschi, C. Mazzuca, T. Coviello, F. Alhaique, and G. Marletta, *J. Phys. Chem. B* **112** (2008) 6473.
20. T. Coviello, L. Bertolo, P. Matricardi, A. Palleschi, G. Bocchinfuso, and F. Alhaique, *Colloid. Polym. Sci.* **287** (2009) 47.
21. G. Bocchinfuso, C. Mazzuca, C. Sandolo, S. Margheritelli, F. Alhaique, T. Coviello, and A. Palleschi, *J. Phys. Chem. B* **114** (2010) 13059.
22. P. Frid, S. V. Anisimov, and N. Popovic, *Brain Res. Rev.* **53** (2007) 135.
23. J. I. Fariña, F. Sñeriz, M. O. Maolina, and N. I. Perotti, *Carbohydr. Polym.* **44** (2001) 41.
24. P. J. Wood, *Carbohydr. Res.* **85** (1980) 271.
25. K. Ogawa and M. Hatano, *Carbohydr. Res.* **67** (1978) 527.
26. K. Ogawa, T. Dohmaru, and T. Yui, *Biosci. Biotech. Bioch.* **58** (1994) 1870.
27. J. O. Duus, C. H. Gotfredsen, and K. Bock, *Chem. Rev.* **100** (2000) 4589.
28. S. Pronk, S. Pall, R. Schulz, P. Larsson, P. Bjelkmar, R. Apostolov, M. R. Shirts et al., *Bioinformatics* **29** (2013) 845.
29. M. Król, T. Borowski, I. Roterman, B. Piekarska, B. Stopa, J. Rybarska, and L. Konieczny, *J. Comput. Aid. Mol. Des.* **18** (2004) 41.

30. U. Essmann, L. Perera, M. L. Berkowitz, T. Darden, H. Lee, and L. G. J. Pedersen, *Chem. Phys.* **103** (1995) 8577.
31. H. J. C. Berendsen, J. P. M. Postma, A. Di Nola, and J. R. J. Haak, *Chem. Phys.* **81** (1984) 3684.
32. H. J. C. Berendsen, J. P. M. Postma, W. F. van Gunsteren, and J. Hermans, in: *Intermolecular Forces*, Pullman, B. (Ed.), D. Reidel Publishing Company, Dordrecht (1981) 331.
33. A. Vishnyakov, A. P. Lyubartsev, and J. Laaksonen, *J. Phys. Chem. A* **105** (2001) 1702.
34. E. F. Pettersen, T. D. Goddard, C. C. Huang, G. S. Couch, D. M. Greenblatt, E. C. Meng, and T. E. Ferrin, *J. Comput. Chem.* **25** (2004) 1605.
35. S. A. Ansari, P. Matricardi, C. Di Meo, F. Alhaique, and T. Coviello, *Molecules* **17** (2012) 2283.
36. T. Yanaki, T. Norisuye, and H. Fujita, *Macromolecules* **13** (1980) 1462.
37. T. Hjerde, B. T. Stokke, O. Smidsrød, and B. E. Christensen, *Carbohydr. Polym.* **37** (1998) 41.
38. X. Leng, K. Starchev, and J. Buffle, *Biopolymers* **59** (2001) 290.